HHS Public Access

Author manuscript

J Heat Transfer. Author manuscript; available in PMC 2019 December 06.

Published in final edited form as:

J Heat Transfer. 2017 March ; 139(3): . doi:10.1115/1.4034962.

Uncertainty Analysis of the Core Body Temperature Under Thermal and Physical Stress Using a Three-Dimensional Whole Body Model

Robins T. Kalathil,
Department of Mechanical and Materials Engineering, University of Cincinnati, Cincinnati, OH 45221

Gavin A. D'Souza,
Department of Mechanical and Materials Engineering, University of Cincinnati, Cincinnati, OH 45221

Amit Bhattacharya,
Department of Environmental Health, University of Cincinnati, Cincinnati, OH 45267

Rupak K. Banerjee[1]
Department of Mechanical and Materials Engineering, University of Cincinnati, 593 Rhodes Hall, Cincinnati, OH 45221

Abstract

Heat stress experienced by firefighters is a common consequence of extreme firefighting activity. In order to avoid the adverse health conditions due to uncompensable heat stress, the prediction and monitoring of the thermal response of firefighters is critical. Tissue properties, among other parameters, are known to vary between individuals and influence the prediction of thermal response. Further, measurement of tissue properties of each firefighter is not practical. Therefore, in this study, we developed a whole body computational model to evaluate the effect of variability (uncertainty) in tissue parameters on the thermal response of a firefighter during firefighting. Modifications were made to an existing human whole body computational model, developed in our lab, for conducting transient thermal analysis for a firefighting scenario. In conjunction with nominal (baseline) tissue parameters obtained from literature, and physiologic conditions from a firefighting drill, the Pennes bioheat and energy balance equations were solved to obtain the core body temperature of a firefighter. Subsequently, the uncertainty in core body temperature due to variability in the tissue parameters (input parameters), metabolic rate, specific heat, density, and thermal conductivity was computed using the sensitivity coefficient method. On comparing the individual effect of tissue parameters on the uncertainty in core body temperature, the metabolic rate had the highest contribution (within ±0.20°C) followed by specific heat (within ±0.10°C), density (within ±0.07°C), and finally thermal conductivity (within ±0.01 °C). A maximum overall uncertainty of ±0.23 °C in the core body temperature was observed due to the combined uncertainty in the tissue parameters. Thus, the model results can be used to effectively predict a realistic range of thermal response of the firefighters during firefighting or similar activities.

[1]Corresponding author. Rupak.Banerjee@uc.edu.

Keywords

uncertainty analysis; whole body model; core body temperature; tissue parameters; firefighting

Introduction

Firefighters often perform strenuous physical activity while enduring intense heat during firefighting scenario. Heat generated by the body, compounded by the ineffective heat dissipation away from the body due to the presence of firefighting protective ensemble, causes heat stress in the body [1]. Heat stress, and the consequent elevation in body temperature, increases the heat strain. This can lead to adverse health effects, including unconsciousness and cardiac arrest. Thus, the accurate prediction of thermal response of the human body during firefighting scenarios is of high importance.

Significance of Tissue Parameters.

Multiple factors are known to have an effect on the thermal response including physical characteristics of the human body, body dynamics, as well as environmental conditions. In particular, tissue parameters such as metabolic rate, $\dot{q}$, specific heat, c, density, ρ, thermal conductivity, k, and blood perfusion, ω, are known to play an important role in the determination of thermal response in the human body [2]. More importantly, these tissue parameters show significant variation among different individuals at resting condition [2–5]. Therefore, an accurate estimation of the thermal response computed over a physiologic range of tissue parameters is critical for preventing an adverse or fatal condition during firefighting.

Evaluation of Tissue Parameters.

A number of studies have listed the physical parameters of tissues. For example, several studies have reported the values of thermal conductivity [6–9], specific heat [7,10,11], density [12–15], and metabolic rate [16,17] of human tissue. Furthermore, comprehensive databases of tissue parameters obtained by consolidating the values reported in literature are also available. An extensive review of physical properties of mammalian tissue, mainly thermal conductivity, specific heat, and thermal diffusivity, has been conducted by Duck [4]. Along with the physical properties of tissues, the techniques for the measurement of these properties have also been discussed in the study. Further, McIntosh and Anderson [2,3] conducted a comprehensive review of tissue parameters of humans at rest condition. The values and the statistical information about the spread of data for the parameters, $\dot{q}$, c, ρ, k, and ω of a number of tissues were quantified. These data can be utilized as inputs to computational models to analyze the temperature distribution in the human body.

Computational Analysis.

Computational analysis is an effective means for conducting a parametric study; such analysis provides the flexibility to manipulate the geometry and physiological parameters of the human body and simulate adverse events like unfavorable environmental conditions. The earliest computational thermal model was developed by Pennes [18] to predict the

temperature distribution in a human arm. Subsequently, several whole body computational models were developed for several applications, including firefighting applications and incorporated the Pennes' bioheat equation to assess the temperature distribution. A predictive heat strain (PHS) model [19] was developed to evaluate the physiological responses of human subjects while wearing different protective garments, which included a firefighting suit. The temperature predicted after walking on a treadmill at 1.25 m/s for 63 min was found to be 1.8 °C higher than the observed value [19]. Further, a thermoregulatory model to predict the skin and core temperatures in firefighters was developed by Kim et al. [20]. The study compared the temperatures predicted by the model with the thermal responses of subjects who had worn the firefighting suit while exercising. A maximum difference of 0.6 °C was observed between the computed and experimentally obtained core temperatures. Although these studies predicted the thermal response of firefighters, *they failed to analyze the effect of variation in tissue parameters on the body temperature*.

More recently, a few numerical studies have assessed the effect of variation in tissue parameters on the temperature distribution in different regions of the human body. A heat transfer model of the skin tissue was developed by Cetingul and Herman [21] for the detection of lesions by analyzing the transient thermal response of the skin layers. The effect of variation in $\dot{q}$, c, k, ω and thickness of the skin layers on the surface temperature distribution were investigated in this study. As the variations in these parameters were less for the skin layers, the corresponding variability in temperature was also found to be less. A human brain electromagnetic-thermal dosimetry model was developed by Cvetković et al. [22]. The temperature rise due to the absorption of the electromagnetic energy and the sensitivity of steady-state temperature to the variations in tissue parameters was assessed. The parameters considered for the sensitivity analysis were the arterial blood temperature, tissue parameters like $\dot{q}$, ω, and k, and boundary conditions like heat transfer coefficient and ambient temperature. *However, these studies focus on only specific regions in the human body and not on the whole body*.

Our group previously developed a whole body computational model to analyze the thermal response of humans at exercise and cold water immersion scenarios [23–25]. We further modified the whole body computational model [23] to predict the thermal response of a firefighter during a firefighting training drill [26,27]. Using this computational model in conjunction with available physiologic tissue parameters obtained from literature, we conducted an uncertainty quantification analysis to evaluate the effect of variability in tissue parameters on the numerical core body temperature, T_{c_N}. *The objective of this research was to determine the uncertainty in* T_{c_N} *due to (1) individual and (2) combined variability in tissue parameters*: $\dot{q}$, c, ρ, *and* k.

Methods

Details of the firefighting drill, the computational model, and the methodology used for conducting the uncertainty analysis are described in the following paragraphs.

Firefighting Training Drill.

Experimental data from the previous studies describing a firefighting training drill were used to develop the human whole body computational model. A typical training drill consisted of alternating firefighting scenarios and rest periods [28,29]. The firefighting scenarios consisted of (1) search for the origin of flame, (2) hose advancement, and (3) search and rescue of the victim. De-identified datasets including the heart rate, experimental core body temperature (T_{c_E}), and physiological details of a single firefighter (age = 33 yr, weight = 86.7 kg) were obtained from Mani et al. [29] and used in this study. The experimental study, conducted by Mani et al. [29], was approved by University of Cincinnati Institutional Review Board and the firefighter provided informed consent prior to participating in the study. The T_{c_E} was measured using a radio pill (CoreTemp, HQ, Inc., Palmetto, FL)., which was ingested by the firefighter prior to the drill. The heart rate of the firefighter was recorded at an interval of 20 s. Figure 1 represents the experimentally obtained heart rate values of the firefighter recorded during the firefighting training drill. In the figure, "Sc" represents the firefighting scenario and "*R*" represents the rest periods.

Whole Body Geometry and Firefighting Suit.

The 3D whole body computational model, shown in Fig. 2(*a*), comprised of several geometric shapes including cylinders, cuboids, and a sphere to represent the limbs, torso, and head, respectively [23,26]. Four domains constituted the whole body model: head, muscle, organ, and gut. An additional suit layer was incorporated to simulate the effects of the firefighting suit at extreme atmospheric conditions. The firefighting suit, comprising of a jacket covering the torso and hands, and pants covering the legs, was modeled as an external layer of 7 mm thickness (Fig. 2(*a*)). The 3D model with the entire firefighting suit layer was used for computations throughout the firefighting scenario while the model ignored the influence of the suit (jacket layer) for computations during the rest periods.

Governing Equations.

Based on the previous model developed by our group [23], the Pennes' bioheat equation and the energy balance equation (please see Eqs. (A1) and (A2) in the Appendix section) were simultaneously solved in order to determine the thermal response of the whole body. For the firefighting application evaluated in this study, additional modifications were made to the previous model which are described below.

Tissue and Firefighting Suit Properties.

All the tissues and organs were categorized into four groups corresponding to four domains (head, organ, muscle, gut) of the whole body model. Details of the tissue parameters including the mean values and percentage uncertainties are presented in Tables 1 and 2. The metabolic rate and perfusion for each domain were determined by calculating the mass weighted average of metabolic rate and perfusion values of all the tissues (e.g., heart, lungs, liver, etc.) belonging to each domain. Further, the mass weighted average value of thermal conductivity, k, specific heat, c, and density, ρ, were computed for the whole body. Since each tissue property had a range of values, the minimum, maximum, and nominal (baseline)

mass weighted average tissue property value for a domain/body were calculated using Eqs. (1)–(3), respectively.

$$X_{\min} = \frac{\sum x_{\min,\,\text{tissue}}\, m_{\text{tissue}}}{\sum m_{\text{tissue}}} \tag{1}$$

$$X_{\max} = \frac{\sum x_{\max,\,\text{tissue}}\, m_{\text{tissue}}}{\sum m_{\text{tissue}}} \tag{2}$$

$$X_n = \frac{X_{\min} + X_{\max}}{2} \tag{3}$$

$$u_x = X_n - X_{\min} = X_{\max} - X_n \tag{4}$$

The minimum and maximum value of any property of an individual tissue are xmin,tissue and xmax,tissue, respectively, and mtissue is the mass of the individual tissue. The (experimental) uncertainty, u_x, of a tissue property was calculated using Eq. (4).

It may be noted that the uncertainty in metabolic rate was determined by assessing the resting metabolic rate of the whole body for different subjects [17]. In order to determine the resting metabolic rate for each domain of the whole body model, the resting metabolic rate values of individual tissues (e.g., heart, lungs, liver, etc.) [2,3,16] were utilized. The mass-weighted average metabolic rate calculated using this method was about 3200 kcal/day. However, this value was found to be higher than the physiologic average metabolic heat generation of 2000 kcal/day (96.85 W), reported [23,30,31] for a resting human being. Therefore, the metabolic rate value of each domain was scaled down to obtain the physiologic average energy consumption value. Corresponding to the two sets of metabolic rate values, two numerical core body temperatures were determined: $T^*_{c\_N}$, based on the metabolic rate values obtained from literature, $\dot{q}^*$, and T_{c_N}, based on the scaled-down metabolic rate values, $\dot{q} \cdot T^*_{c\_N}$ and T_{c_N} in the current study were defined as the average tissue temperature of the gut region. The material properties of the firefighting suit were unavailable and were considered as proprietary information. Therefore, the material properties of the suit were based on the literature [32,33] and are reported in Table 3.

Instantaneous Metabolic Rate.

The instantaneous metabolic rate, $\dot{q}_m$, in the Pennes' equation (Eq. (A1) in the Appendix) is given by [34]

$$\dot{q}_m = \left(\sum \dot{q}_i V_i + \frac{(\text{HR} - \text{HR}_0)\text{BSA}}{\text{RM}} \right) \left(\frac{1}{V_{\text{body}}} \right) \tag{5}$$

where $\dot{q}_i$ and V_i are the resting volumetric metabolic rate and volume of individual domain, respectively; HR is the current heart rate; HR_0 is the experimentally recorded initial heart rate; RM is the increase in heart rate per unit metabolic rate; and BSA is the body surface area. RM and BSA are defined as

$$RM = \frac{HR_{max} - HR_0}{MWC - \left(\frac{\sum \dot{q}_i V_i}{BSA}\right)} \tag{6}$$

$$BSA = 0.202 * W^{0.425} h^{0.725} \tag{7}$$

where HR_{max} is the maximum heart rate and MWC is the maximum working capacity defined as

$$HR_{max} = 205 - (0.62A) \tag{8}$$

$$MWC = (41.7 - (0.22A))W^{0.666} \tag{9}$$

where A is the age and W is the weight of the firefighter. In the model, 92% of the increase in metabolic rate was transferred to the muscle domain while the remaining was assigned to the organ domain [35]. The perfusion values for muscle and organ were allowed to vary with their respective metabolic rate values. However, perfusion values were limited between 0.0005 and 0.0115 s^{-1} based on the physiologic variation in cardiac output (5–40 L/min).

Cardiac Output and Stroke Volume.

Cardiac output was defined as the volume of blood being pumped by the heart per unit time. This, in the context of the current study, was the volumetric summation of perfusion in the body. Thus, the cardiac output is given by

$$\text{Cardiac Output } = (\omega_{he} \times V_{he}) + (\omega_{mu} \times V_{mu}) + (\omega_{or} \times V_{or}) + (\omega_{gu} \times V_{gu}) \tag{10}$$

where the subscripts “he,” “mu,” “or,” and “gu” refer to the domains, head, muscle, organ, and gut. The stroke volume was calculated by dividing the cardiac output by the heart rate.

Boundary Conditions.

When the increase in perfusion was inadequate to regulate the body temperature, sweating was triggered to increase the removal of excess heat from the muscles [23,26]. This can be expressed as

$$-k_t \frac{\partial T_t}{\partial n}\bigg|_{\text{at surface}} = h(T_t - T_{\text{air}})\big|_{\text{at surface}} + E \tag{11}$$

where n is the normal direction of the skin surface, h is the heat transfer coefficient, and T_{air} is the ambient air temperature. E represents the heat loss due to sweating, which was

calculated as a function of the evaporative heat transfer rate, h_e, and the difference between the vapor pressure of water at the skin temperature, p_{sk}, and the partial pressure of water vapor in the ambient air, p_{air}. Additional details about p_{sk} and p_{air} can be found in our previous study [23]. The expression for E [30] is given as

$$E = 0.1333\left[\frac{\text{kPa}}{\text{mm Hg}}\right] w f_{\text{cl}} h_e \left(p_{\text{sk}} - p_{\text{air}}\right) \tag{12}$$

The skin wettedness factor, w, indicated the amount of skin layer that was covered with sweat and it varies between 0 and 1 [26,30]. The estimation of w is challenging, particularly in events like firefighting as it is dependent on factors such as amount of skin exposure, time, clothing, ambient temperature, removal of sweat using absorbent, and humidity [36]. Therefore, in the present study, the w was calculated based on the slope of T_{c_E} and the duration of the rest periods. The optimized w value of 0 for rest period R1 and 0.3 for rest period R2 was used for the computations [26,27]. The value of the intrinsic clothing thermal efficiency, f_{cl}, [30] was kept at 0.36 [26] for the torso and head regions during the rest periods.

The h and T_{air} values were provided as the boundary conditions to the model. At ambient conditions (T_{air} = 25 °C), the h value of 4.7 W/m^2 °C was iteratively determined by satisfying the steady-state condition [23], wherein, the tissue temperature is equal to initial T_{blood} value of 37 °C.

Uncertainty Analysis.

The whole body model was used to quantify the uncertainty in numerical core body temperatures ($T^*_{c\_N}$ and T_{c_N}) due to variability in the tissue parameters (input parameters).

The sensitivity coefficient method, which is a local approach, was used for conducting the uncertainty analysis [37]. The overall uncertainty in each numerical core body temperature can be calculated by

$$u^2 = \sum_{i=1}^{n} \left(\frac{\partial S}{\partial X_i} u_{x_i}\right)^2 \tag{13}$$

where u is the simulation uncertainty, S is the simulation result ($T^*_{c\_N}$ or T_{c_N}), X_i represents the ith input parameter, $\partial S/\partial X_i$ is the sensitivity coefficient, u_{x_i} is the experimental uncertainty in the ith input parameter, and n is the number of input parameters. The expression for the sensitivity coefficient, obtained using Taylor series expansion, is given as

$$\frac{\partial S}{\partial X_i} = \frac{S\left(X_1 \ldots, X_i + \Delta X_i, \ldots, X_n\right) - S\left(X_1, \ldots, X_i - \Delta X_i, \ldots, X_n\right)}{2\Delta X_i} + O\left(\Delta X_i^2\right) \tag{14}$$

where terms of second-order and higher are truncated, thus resulting in a second-order accurate central difference solution. Each input parameter was perturbed above and below its mean (baseline) value by a relative perturbation size, $\Delta X/X$, of 10^{-4}. This relative

perturbation size was selected based on the recommended values in the ASME V&V 20, 2009 [37] for minimizing the truncation and round-off errors. Subsequently, the T_{c_N} values, computed using the perturbed input parameters, were used to obtain the sensitivity coefficient (Eq. (14)). The uncertainty, u, in T_{c_N} was then calculated using Eq. (13). Thus, the total uncertainty, u, accounts for the perturbation ($\partial S/\partial X_i$) of input parameter and the variability (u_x) in human subjects.

To determine the uncertainty in T_{c_N}, $2n + 1$ computations were performed where n is the number of input parameters. Although four tissue parameters (k, ρ, c, $\dot{q}$) were chosen as input parameters for the uncertainty analysis, a different $\dot{q}$ value was assigned to each of the four domains ($\dot{q}_{\text{he}}$, $\dot{q}_{\text{mu}}$, $\dot{q}_{\text{or}}$, $\dot{q}_{\text{gu}}$) for the computations. Considering each $\dot{q}$ to be a separate input parameter resulted in a total of seven input parameters. The uncertainty in $T^*_{c\_N}$ due to variability in k, ρ, c, and $\dot{q}^*$ was determined by adopting the same methodology.

The Pennes equation (Eq. (A1) in the Appendix) was solved by utilizing a first-order implicit transient scheme which is inherently stable and a second-order spatial discretization scheme. Further, an implicit formulation was employed to solve the energy balance equation (Eq. (A2) in the Appendix) [23]. A fixed time-step size of 20 s was used for a total time of 95 min (285 time-steps) to solve the transient thermal response. This size of the time-step was selected based on the acquisition of heart rate data [29]. Further, the energy residuals were converged to 10^{-10} at each time-step. For each time-step, approximately eight iterations were required for achieving convergence. In addition, a mesh independence study was conducted on the whole body model. The mesh was refined until the change in steady-state temperature was less than 1% at ambient conditions (Fig. 2(*b*)). A total of 340,000 tetrahedral elements were used to discretize the human whole body computational domain. For all the computations, a finite volume solver (FLUENT, ANSYS, Inc., Canonsburg, PA) was used. User-defined functions, written in C programming language, were used to assess the effects of perfusion (Eq. (A1) in the Appendix), solve the energy balance equation (Eq. (A2) in the Appendix), and to compute the instantaneous metabolic rate (Eq. (5)) and heat loss due to sweating (Eq. (12)). Further details regarding the numerical schemes used for solving the governing equations are given in our previous study [23]. The individual uncertainty in T_{c_N} and $T^*_{c\_N}$ was initially evaluated by perturbing each tissue property at a time while keeping other input parameters at baseline values. Subsequently, the overall uncertainly at T_{c_N} and $T^*_{c\_N}$ was obtained by combining the individual uncertainties using Eq. (13).

Results

The transient variations in the core body temperature of the firefighter were determined using a whole body computational model. The T_{c_N} was quantified by accounting for individual and combined effects of variability in tissue parameters: specific heat, c, density, ρ, and conductivity, k, as well as metabolic rate, $\dot{q}$. Additionally, the cardiac output and the stroke volume were also determined.

Temperature Distribution.

The temperature contours at steady-state (prefirefighting scenario) and during a firefighting scenario (t = 60 min) are provided in Figs. 3(*a*) and 3(*b*), respectively. The firefighting training drill of 95 min consisted of alternating firefighting scenarios, Sc, and rest periods, R. The computed steady-state temperature varied between 27.6 °C in the suit layer to 37.5 °C in the internal organs and gut region (Fig. 3(*a*)). Lower temperatures were observed at the surface region of the whole body domain. Nearly uniform temperatures were observed in the inner regions, such as the torso and legs. The T_{c_N}, defined as the average tissue temperature of the gut domain, was observed to be 37.4 °C. As a representative case, Fig. 3(*b*) shows the temperature distribution at the end of the second firefighting scenario (Sc2). The temperature field was found to be somewhat uniform in the inner regions. This is similar to that observed for the steady-state case (Fig. 3(*a*)). However, the temperature increased during the firefighting scenario and varied from 28.0 °C in the suit layer to 38.2 °C in the internal organs and gut. The corresponding T_{c_N} was calculated to be 38.2 °C and was around 2% higher than the steady-state T_{c_N}.

Temporal Variations in the Core Body Temperatures.

The T_{c_E} was compared with the numerical core body temperature, $T^*_{c\_N}$, as shown in Fig. 4(*a*). The $T^*_{c\_N}$ was computed using rest metabolic rate values, $\dot{q}^*$, obtained from previous studies [2,3,16,17]. The variations between $T^*_{c\_N}$ and T_{c_E} were observed to increase at higher temperatures (Fig. 4(*a*)). At Sc3 (t = 95 min), $T^*_{c\_N}$ was 40.0 °C while T_{c_E} was 38.6 °C resulting in a maximum difference of 1.4°C or 3.6% { = [(40.0–38.6)/38.6] × 100%}. A comparison of the numerical core body temperature, T_{c_N}, based on scaled-down metabolic rate, $\dot{q}$, with T_{c_E} is shown in Fig. 4(*b*). A maximum deviation of 0.3 °C or 0.8% {=[(38.3 – 38.0)/38.3] × 100%} was observed at Sc2 (t = 54 min) between T_{c_E} (38.3 °C) and T_{c_N} (38.0 °C). This difference was comparatively better than the difference noted between $T^*_{c\_N}$ and T_{c_E} (Fig. 4(*a*)). Consequently, hereafter in the Results section, the individual uncertainty due to variability in each tissue parameter is reported for T_{c_N} and not for $T^*_{c\_N}$. However, the overall uncertainty is reported for both T_{c_N} and $T^*_{c\_N}$.

Effect of Specific Heat, c, Density, ρ, and Conductivity, k.

The uncertainty in transient T_{c_N} due to variability in c is represented in Fig. 5(*a*). The uncertainty in c was reported to be 6.6% (Table 1). Accounting for this uncertainty, a maximum uncertainty of ±0.10 °C in T_{c_N} was observed (Sc3, t = 95 min). Figure 5(*b*) illustrates the influence of variability in ρ on the transient T_{c_N}. A 4.3% uncertainty in ρ resulted in a maximum uncertainty of ±0.07 °C (Sc3, t = 95min) in T_{c_N}. Figure 5(*c*) illustrates the effect of variation in k on the transient T_{c_N}. A maximum uncertainty of ±0.01 °C in T_{c_N} (Sc3, t = 95min) was observed due to an uncertainty of 6.3% in k. It was observed that the c had more influence on T_{c_N} compared to ρ and k. Furthermore, in the above three cases, the uncertainty in T_{c_N} increased with the elevation in T_{c_N} value. For example, when the T_{c_N} was 38.3 °C, the uncertainty associated with it due to variability in

c was observed to be ±0.06 °C (Fig. 5(*a*)). When the value increased to 38.8 °C, the corresponding uncertainty was ±0.10°C.

Effect of Rest Metabolic Rate, $\dot{q}$.

Figure 6 illustrates the uncertainty in transient T_{c_N} due to variability in $\dot{q}$. As a result of an 18.4% variability in $\dot{q}$, a maximum uncertainty of ±0.20 °C was observed in T_{c_N} (t = 95 min). Uncertainty in T_{c_N} increased when the T_{c_N} value got elevated. For example, the uncertainties in T_{c_N} at the end of Sc1, Sc2, and Sc3 were observed to be ±0.06 °C, ±0.13 °C, and ±0.20°C, respectively. These values corresponded to T_{c_N} values of 37.7 °C, 38.2 °C, and 38.8 °C, respectively. As observed from Figs. 5 and 6, $\dot{q}$ had a greater effect on T_{c_N} in comparison to c, ρ, and k.

Comparison of Uncertainties in T_{c_E} and T_{c_N}.

The overall uncertainty in T_{c_E} and T_{c_N} was compared and analyzed, as shown in Fig. 7(*a*). The T_{c_E} was measured using a temperature measurement system (CoreTemp), which was accurate to ±0.1 °C. This value was considered to be the uncertainty in T_{c_e}. The overall uncertainty in T_{c_N} was calculated by combining the individual uncertainties due to variability in c, ρ, k, and $\dot{q}$ using the sensitivity coefficient method for parameter uncertainty propagation [37]. The overall uncertainties in T_{c_N} at the end of Sc1, Sc2, and Sc3 were ±0.06°C, ±0.14°C, and ±0.23°C, respectively. These values corresponded to r_{cJV} values of 37.7 °C, 38.2 °C, and 38.8 °C. A maximum overall uncertainty of ±0.23 °C was observed at the end of Sc3, corresponding to a T_{c_N} value of 38.8 °C. The T_{c_N} values predicted by the computational model over the entire range of tissue parameters were observed to fall mostly within the range of T_{c_E} values.

Comparison of Overall Uncertainties in $T^*_{c\_N}$ and T_{c_N}.

The overall uncertainties in the two numerical core body temperatures, $T^*_{c\_N}$ (based on the $\dot{q}^*$ values) and T_{c_N} (based on the scaled-down metabolic rate, $\dot{q}$), were compared in Fig. 7(*b*). The methodology adopted for the quantification of uncertainties in $T^*_{c\_N}$ and T_{c_N} was the same. Higher uncertainty was observed in T_{c_N} and $T^*_{c\_N}$ at higher mean values. For example, uncertainty values in $T^*_{c\_N}$ at the end of Sc1, Sc2, and Sc3 were observed to be ±0.08 °C, ±0.27 °C, and ±0.40 °C. This corresponded to $T^*_{c\_N}$ values of 37.9 °C, 38.9 °C, and 40.0 °C, respectively. Additionally, higher uncertainties were observed in compared to T_{c_N}. Maximum uncertainty of ±0.40 °C was observed in $T^*_{c\_N}$ compared to a ±0.23 °C for T_{c_N}. Baseline $T^*_{c\_N}$ showed a maximum deviation of 1.4°C or 3.6% {=[(40.0–38.6)/38.6] × 100%}, from T_{c_E} and 1.2°C or 3.1% {=[(40.0–38.8)/38.8] × 100%} from T_{c_N}, at the end of Sc3.

Cardiac Output and Stroke Volume.

The variation of cardiac output and stroke volume is illustrated in Fig. 8. The cardiac output varied from 5.5 L/min to 12.5 L/min and the stroke volume varied between 0.06 L/beat and 0.08 L/beat during the entire firefighting activity. Higher cardiac output and stroke volume were observed during the firefighting scenarios compared to the preceding rest scenarios. For example, the maximum cardiac output observed during Sc2 was 11.5 L/min and that observed during R1 was 7.7 L/min. Similarly, the maximum stroke volume observed during Sc2 was 0.077 L/beat and that observed during R1 was 0.066 L/beat.

Discussion

The variability in tissue parameters is observed to have an effect on the core body temperature of firefighters during firefighting. This effect can be quantified using a whole body computational model as demonstrated in the results above. Using the sensitivity coefficient method for uncertainty analysis, we could assess the influence of individual and combined variability in tissue parameters on T_{c_N}.

Temperature Distribution.

From the results (Fig. 3(*a*)), the metabolic rate is observed to influence the steady-state temperature distribution in the human body. Elevated temperatures were observed in the inner zones (organ and gut) due to the higher metabolic rate in these domains. Similarly, higher temperature values were observed in the head due to the increased metabolic rate in the brain. However, the muscle and the suit layer exhibited reduced temperatures due to a lower metabolic rate and the ambient boundary condition, respectively.

Core Body Temperatures.

In our previous study [23], the numerical core body temperature was defined as the average tissue temperature (T_t) of the "organ" domain. However, in the current study, the whole body model was subdivided to include an exclusive "gut" domain which was enclosed within the organ domain. The average temperature in this domain was computed as the core body temperature. We assume that this modification could enhance the comparison between the numerical and experimental core body temperatures due to an improved localized averaging of the numerical core body temperature.

Variations in Core Body Temperatures.

An increase in T_{c_N} was observed at all scenarios. This can be attributed to the continuous heat generation in the tissues, and ineffective heat dissipation from the body due to the presence of the suit layer (Figs. 4(*a*) and 4(*b*)). The suit layer, comprising of a "jacket" and "pants," was worn throughout the firefighting scenarios (Sc1, Sc2, and Sc3). However, the jacket was removed by the firefighter during the rest periods (R1 and R2). This could be one of the reasons for the observed reduction in temperature rise during R1 and R2 (Figs. 4(*a*) and 4(*b*)). Further, variations were observed between the trends of T_{c_E} and T_{c_N}. Specifically, there was a delay in time rate of change of T_{c_N} compared to that in T_{c_E}. One of the reasons for the delay could be a lower thermal diffusivity adopted in the numerical analysis.

Effect of Variability in Input Parameters on T_{c_N}.

The variability in the $\dot{q}$ contributed highest toward the overall uncertainty in T_{c_N}. One of the reasons for this effect is the higher variability in $\dot{q}$ (18.4%) compared to the variability in c (6.6%), ρ (4.3%), and k (6.3%). Furthermore, the uncertainty in $\dot{q}$ had an effect on the instantaneous metabolic rate, $\dot{q}_m$, which, in turn, influenced the T_{c_N} [26,27]. This could be another reason for the higher effect of variability in $\dot{q}$ on the uncertainty in T_{c_N}.

Cardiac Output and Stroke Volume.

The cardiac output and the stroke volume obtained in the current study were mostly within the physiological range [26]. It may be noted that a decrease in both cardiac output and stroke volume was observed at the end of firefighting scenarios 2 and 3 (Sc2 and Sc3). The stroke volume was determined from the cardiac output and the heart rate. While the cardiac output was associated with the overall perfusion in the body, the perfusion in the organ and muscle varied with their respective metabolic rates. Therefore, a better correlation between the perfusion and the metabolic rate could help in improving the determination of cardiac output and stroke volume.

Limitations.

The following limitations have been identified which may change the outcomes reported above.

The whole body model assumed a constant value of ambient temperature (T_{air} = 25°C) and heat transfer coefficient (h = 4.7 W/m^2°C). However, these parameters can vary in realistic conditions [30].

The *range of parameter values of several tissues* was based on studies [2,3] conducted using limited number of subjects (n<10). Evaluating the data of a larger group of human subjects may lead to a more accurate estimation of the range of tissue parameters. The accuracy of the tissue parameters can be improved by conducting a more comprehensive analysis of individual tissues in the human body. The weighted average and overall ranges of values of tissue parameters were calculated based on a fixed mass of tissues [5], while the percentage content of different types of tissues in the human body (for example, fat/muscle content) and the weight of tissues may vary from person to person. In other words, knowledge of firefighter-specific tissue parameters is expected to improve the prediction of T_{c_N}. Further, the variation of c, ρ, and k with temperature has not been accounted for in the present study.

The average $\dot{q}^*$ of 3200 kcal/day (unsealed) calculated based on individual tissue values [2,3,16] was higher (~60%) than the reported average value of 2000 kcal/day (scaled) for a resting human being [23,30,31]. The *resting $\dot{q}^*$ for the firefighter* could be higher, and it may influence the transient variation in $\dot{q}^*$ with respect to the heart rate, which has been accounted for in this formulation. Therefore, incorporation of improved resting $\dot{q}^*$ specific to individual firefighter could lead to a better comparison between the T_{c_E} and T_{c_N}.

In the future, evaluating the effect of the variations in ambient conditions, properties of the firefighting suit, and the variation of tissue parameters with temperature can further enhance

the applicability of the whole body model. Further, data-driven models have been reported to be effective for short-term prediction of the T_{c_N} of individual firefighters [38,39]. Therefore, individualized prediction of the T_{c_N} for a firefighter could be improved by developing hybrid models which combines the strength of the whole body model and the utility of data-driven predictive models.

Conclusion

The current study evaluated the effect of variability in tissue parameters on T_{c_N} of a firefighter using the whole body computational model. The uncertainty quantification facilitated in predicting a realistic range of T_{c_N} during firefighting by accounting for the natural variability in tissue parameters among the human population. Based on the results, variability in $\dot{q}$ had the maximum contribution toward the overall uncertainty in T_{c_N} while variability in k was found to have the least effect on it. The applicability of the whole body computational model can be further extended to determine the T_{c_N} under different environmental factors and physiological conditions of individuals. Based on the model results, firefighters, athletes, and other personnel could be informed of when they should stop exercising to prevent health problems that arise due to higher thermal stress. This can be achieved using minimal real time data from the subject.

Acknowledgment

The authors would like to acknowledge Mr. Anup Paul who developed the initial subroutine for the whole body model [23]. The whole body model for firefighters developed in this study is an improvement over a similar model developed by Mr. Swarup Zachariah in his M.S. thesis [26]. The authors would also like to thank Mr. Anup Paul and Mr. Swarup Zachariah for (a) assisting in transitioning the research, and (b) providing initial inputs for the present study.

This study was partially supported by the National Institute for Occupational Safety and Health (NIOSH) Pilot Research Project (PRP) Training Program of the University of Cincinnati Education and Research Center Grant No. #T42/OH008432-08.

Appendix

This section includes the governing equations of the whole body model which was previously developed by Paul et al. [23]. The transient thermal response of the whole body was determined by solving two equations simultaneously: (1) the Pennes' bioheat equation, to calculate the tissue temperature of the body and (2) the energy balance equation, to evaluate the change in blood temperature due to tissue-blood heat exchange. The Pennes' equation is defined as

$$\rho_t c_t \frac{\partial T_t}{\partial t} = k_t \nabla^2 T_t + \dot{q}_m + \rho_{\text{blood}} C_{\text{blood}} \omega \left(T_{\text{blood}} - T_t\right) \quad \text{(A1)}$$

where subscripts "t" and "blood" represent the properties of tissue and blood, respectively, T represents the temperature and $\dot{q}_m$ is the volumetric metabolic heat generation. The T_{blood} was represented as a lumped parameter and is computed using the energy balance equation, given as

$$\rho_{\text{blood}}\, c_{\text{blood}}\, V_{\text{blood}} \frac{dT_{\text{blood}}}{dt} = -\rho_t c_t \omega_{\text{avg}}\, V_{\text{body}} \left(T_{\text{blood}} - T_{\text{wt}}\right) \tag{A2}$$

where V_{body} is the combined volumes of all the domains of the human body. The volumetric average blood perfusion rate per unit volume of tissue, ω_{avg}, and the perfusion weighted average tissue temperature, T_{wt}, are defined as

$$\omega_{\text{avg}} = \frac{1}{V_{\text{body}}} \iiint_{V_{\text{body}}} \omega dV_{\text{body}} \tag{A3}$$

$$T_{\text{wt}} = \frac{1}{\omega_{\text{avg}} V_{\text{body}}} \iiint_{V_{\text{body}}} \omega T_t dV_{\text{body}} \tag{A4}$$

Nomenclature

A	age (yr)
BSA	body surface area (m^2)
c	specific heat capacity (J/kg °C)
E	heat loss due to sweating (W/m^2)
f	intrinsic thermal efficiency (dimensionless)
h	overall heat transfer coefficient (W/m^2 °C)
HR	heart rate (beats/min)
k	thermal conductivity (W/m °C)
m	mass (kg)
MWC	maximum working capacity (W/m^2)
p	vapor pressure of water (mm Hg)
$\dot{q}$	scaled-down resting metabolic rate (W/m^3)
$\dot{q}_m$	instantaneous metabolic rate (W/m^3)
$\dot{q}^*$	resting metabolic rate obtained from literature (W/m^3)
R	rest period
RM	increase in metabolic rate per unit heart rate (beats m^2/W min)
S	simulation result

Sc	firefighting scenario
t	time (s)
T	temperature (°C)
T_c	core body temperature
T_{c_E}	experimental core body temperature
T_{c_N}	numerical core body temperature based on $\dot{q}$
$T^*_{c\_N}$	numerical core body temperature based on $\dot{q}^*$
u	simulation uncertainty
u_{x_i}	experimental uncertainty of a tissue property
V	volume (m^3)
w	amount of generated sweat available for evaporation
W	weight of the firefighter (kg)
X	mass weighted average value of tissue property
$x_{min,tissue}$	minimum value of any tissue property
$x_{max,tissue}$	maximum value of any tissue property

Greek Symbols

ρ	density (kg/m^3)
ω	blood perfusion rate (1/s)

Subscripts

air	air
avg	average
blood	blood
cl	clothing
e	evaporative
gu	gut
he	head
max	maximum

min	minimum
mu	muscle
n	nominal (baseline)
or	organ
sk	skin
t	tissue
wt	perfusion weighted average
0	rest (initial)

References

[1]. Budd GM, Brotherhood J, Hendrie A, Jeffery S, Beasley F, Costin B, Zhien W, Baker M, Cheney N, and Dawson M, 1997, "Project Aquarius 1. Stress, Strain, and Productivity in Men Suppressing Australian Summer Bush-fires With Hand Tools: Background, Objectives, and Methods," Int. J. Wildland Fire, 7(2), pp. 69–76.

[2]. Mcintosh RL, and Anderson V, 2010, "A Comprehensive Tissue Properties Database Provided for the Thermal Assessment of Human at Rest," Biophys. Rev. Lett, 05(03), pp. 129–151.

[3]. Mcintosh RL, and Anderson V, 2013, "Erratum: 'A Comprehensive Tissue Properties Database Provided for the Thermal Assessment of a Human at Rest,'" Biophys. Rev. Lett, 08(01n02), pp. 99–100.

[4]. Duck FA, 1990, Physical Properties of Tissue: A Comprehensive Reference Book, Academic Press, London.

[5]. Werner J, and Buse M, 1988, "Temperature Profiles With Respect to Inhomogeneity and Geometry of the Human Body," J. Appl. Physiol. (Bethesda, Md.: 1985), 65(3), pp. 1110–1118.

[6]. Bowman HF, 1981, "Heat Transfer and Thermal Dosimetry," J. Microwave Power, 16(2), pp. 121–133.

[7]. Cooper TE, and Trezek GJ, 1972, "A Probe Technique for Determining the Thermal Conductivity of Tissue," ASME J. Heat Transfer, 94(2), pp. 133–140.

[8]. Cooper TF, and Trezek GJ, 1971, "Correlation of Thermal Properties of Some Human Tissue With Water Content," Aerosp. Med, 42(1), pp. 24–27. [PubMed: 5541087]

[9]. Poppendiek HF, Randall R, Breeden JA, Chambers JE, and Murphy JR, 1967, "Thermal Conductivity Measurements and Predictions for Biological Fluids and Tissues," Cryobiology, 3(4), pp. 318–327.

[10]. El-Brawany MA, Nassiri DK, Terhaar G, Shaw A, Rivens I, and Lozhken K, 2009, "Measurement of Thermal and Ultrasonic Properties of Some Biological Tissues," J. Med. Eng. Technol, 33(3), pp. 249–256. [PubMed: 19340696]

[11]. Henriques FC, and Moritz AR, 1947, "Studies of Thermal Injury: I. The Conduction of Heat to and Through Skin and the Temperatures Attained Therein. A Theoretical and an Experimental Investigation," Am. J. Pathol, 23(4), pp. 530–549. [PubMed: 19970945]

[12]. Behnke AR, 1961, "Comment on the Determination of Whole Body Density and a Resume of Body Composition Data," Techniques for Measuring Body Composition, Brozek J and Henschel A, eds., National Academy of Sciences/National Research Council, Washington, DC, p. 118.

[13]. Brozek J, 1952, "Changes of Body Composition in Man During Maturity and Their Nutritional Implications," Fed. Proc, 11(3), pp. 784–793. [PubMed: 12980132]

[14]. Krzywicki HJ, and Chinn KS, 1967, "Human Body Density and Fat of an Adult Male Population as Measured by Water Displacement," Am. J. Clin. Nutr, 20(4), pp. 305–310. [PubMed: 6022006]

[15]. Pascal LR, Grossman MI, Sloane HS, and Frankel T, 1956, “Correlations Between Thickness of Skinfolds and Body Density in 88 Soldiers,” Hum. Biol, 28(2), pp. 165–176. [PubMed: 13353957]

[16]. Elia M, 1992, “Organ and Tissue Contribution to Metabolic Rate,” Energy Metabolism: Tissue Determinants and Cellular Corollaries, Raven Press, New York, pp. 19–60.

[17]. Weinsier RL, Schutz Y, and Bracco D, 1992, “Reexamination of the Relationship of Resting Metabolic Rate to Fat-Free Mass and to the Metabolically Active Components of Fat-Free Mass in Humans,” Am. J. Clin. Nutr, 55(4), pp. 790–794. [PubMed: 1550060]

[18]. Pennes HH, 1948, “Analysis of Tissue and Arterial Blood Temperatures in the Resting Human Forearm,” J. Appl. Physiol, 1(2), pp. 93–122. [PubMed: 18887578]

[19]. Wang F, Kuklane K, Gao C, and Holmer I, 2011, “Can the PHS Model (IS07933) Predict Reasonable Thermophysiological Responses While Wearing Protective Clothing in Hot Environments?,” Physiol. Meas, 32(2), pp. 239–249. [PubMed: 21178244]

[20]. Kim JH, Williams WJ, Coca A, and Yokota M, 2013, “Application of Thermoregulatory Modeling to Predict Core and Skin Temperatures in Firefighters,” Int. J. Ind. Ergon, 43(1), pp. 115–120.

[21]. Cetingul MP, and Herman C, 2010, “A Heat Transfer Model of Skin Tissue for the Detection of Lesions: Sensitivity Analysis,” Phys. Med. Biol, 55(19), pp.5933–5951. [PubMed: 20858919]

[22]. Cvetković M, Poljak D, and Hirata A, 2016, “The Electromagnetic-Thermal Dosimetry for the Homogeneous Human Brain Model,” Eng. Anal. Boundary Elem, 63, pp. 61–73.

[23]. Paul AK, Zachariah S, Zhu L, and Banerjee RK, 2015, “Predicting Temperature Changes During Cold Water Immersion and Exercise Scenarios: Application of a Tissue-Blood Interactive Whole-Body Model,” Numer. Heat Transfer, Part A, 68(6), pp. 598–618.

[24]. Paul AK, Zachariah SA, Zhu L, and Banerjee RK, 2013, “Theoretical Predictions of Body Tissue and Blood Temperature During Cold Water Immersion Using a Whole Body Model,” ASME Paper No. SBC2013–14398.

[25]. Zachariah SA, Paul AK, Banerjee RK, and Zhu L, 2013, “Influence of Exercise Condition on Tissue Blood Temperature Using Whole Body Model,” ASME Paper No. SBC2013–14515.

[26]. Zachariah S, 2015, “Methodology to Predict Core Body Temperature, Cardiac Output, and Stroke Volume for Firefighters Using a 3D Whole Body Model,” Master thesis, University of Cincinnati, Cincinnati, OH.

[27]. Zachariah SA, 2015, “Prediction of Core Body Temperature Sweat Rate Cardiac Output and Stroke Volume for Firefighters Using a 3D Whole Body Model,” ASME J. Biomech. Eng, 137(2), p. 020207.

[28]. Horn GP, Blevins S, Fernhall B, and Smith DL, 2013, “Core Temperature and Heart Rate Response to Repeated Bouts of Firefighting Activities,” Ergonomics, 56(9), pp. 1465–1473. [PubMed: 23869685]

[29]. Mani A, Musolin K, James K, Kincer G, Alexander B, Succop P, Lovett W, Jetter WA, and Bhattacharya A, 2013, “Risk Factors Associated With Live Fire Training: Buildup of Heat Stress and Fatigue, Recovery and Role of Micro-Breaks,” Occup. Ergon, 11(2), pp. 109–121.

[30]. Handbook A, 2009, ASHRAE Handbook-Fundamentals, American Society of Heating, Refrigerating and Air-Conditioning Engineers, Inc., Atlanta, GA.

[31]. Zhu L, Schappeler T, Cordero-Tumangday C, and Rosengart A, 2009, “Thermal Interactions Between Blood and Tissue,” Advances in Numerical Heat Transfer, Vol. 3, CRC Press, New York.

[32]. Lawson JR, Walton WD, Bryner NP, and Amon FK, 2005, “Estimates of Thermal Properties for Fire Fighters’ Protective Clothing Materials,” U.S. Department of Commerce, National Institute of Standards and Technology, Gaithersburg, MD.

[33]. Prasad K, Twilley WH, and Lawson JR, 2002, “Thermal Performance of Fire Fighters’ Protective Clothing: Numerical Study of Transient Heat and Water Vapor Transfer,” U.S. Department of Commerce, Technology Administration, National Institute of Standards and Technology, Gaithersburg, MD.

[34]. ISO, 2004, “Ergonomics of the Thermal Environment-Determination of Metabolic Rate,” BSI, London, Standard No. ISO 8996:2004.

[35]. Despopoulos A, and Silbernagl S, 2003, Color Atlas of Physiology, Thieme Stuttgart, New York.

[36]. Malchaire J, Piette A, Kampmann B, Mehnert P, Gebhardt H, Havenith G, Den Hartog E, Holmer I, Parsons K, and Alfano G, 2001, "Development and Validation of the Predicted Heat Strain Model," Ann. Occup. Hyg, 45(2), pp. 123–135. [PubMed: 11182426]

[37]. The American Society of Mechanical Engineers, 2009, "Standard for Verification and Validation in Computational Fluid Dynamics and Heat Transfer," ASME, New York, Standard No. V V 20–2009.

[38]. Gribok AV, Buller MJ, and Reifman J, 2008, "Individualized Short-Term Core Temperature Prediction in Humans Using Biomathematical Models," IEEE Trans. Biomed. Eng, 55(5), pp. 1477–1487. [PubMed: 18440893]

[39]. Mani A, Rao M, James K, and Bhattacharya A, 2015, "Individualized Prediction of Heat Stress in Firefighters: A Data-Driven Approach Using Classification and Regression Trees," J. Occup. Environ. Hyg, 12(12), pp. 845–854. [PubMed: 26170240]

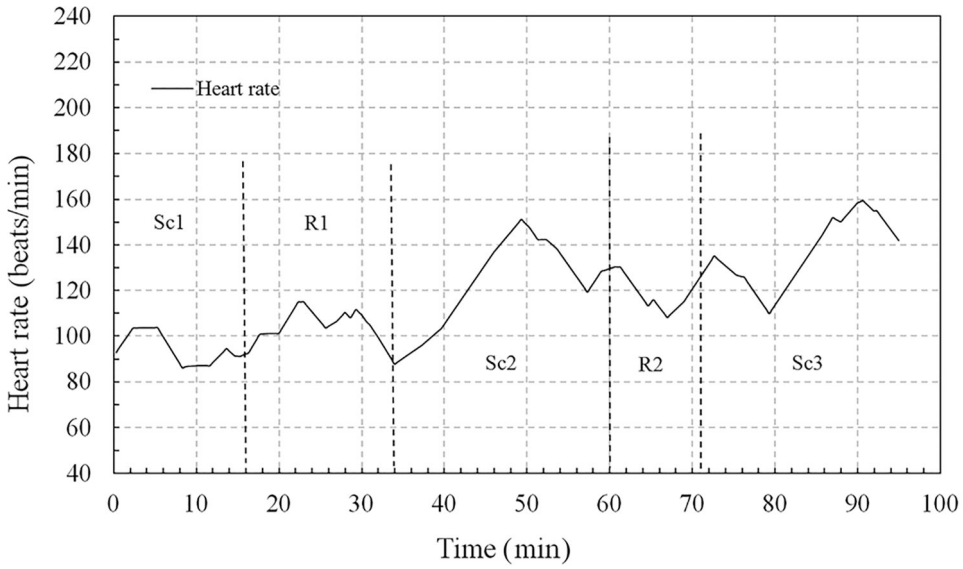

Fig. 1.

The heart rate data of a firefighter during the entire firefighting training drill comprising of work (Sc) and rest (*R*) conditions

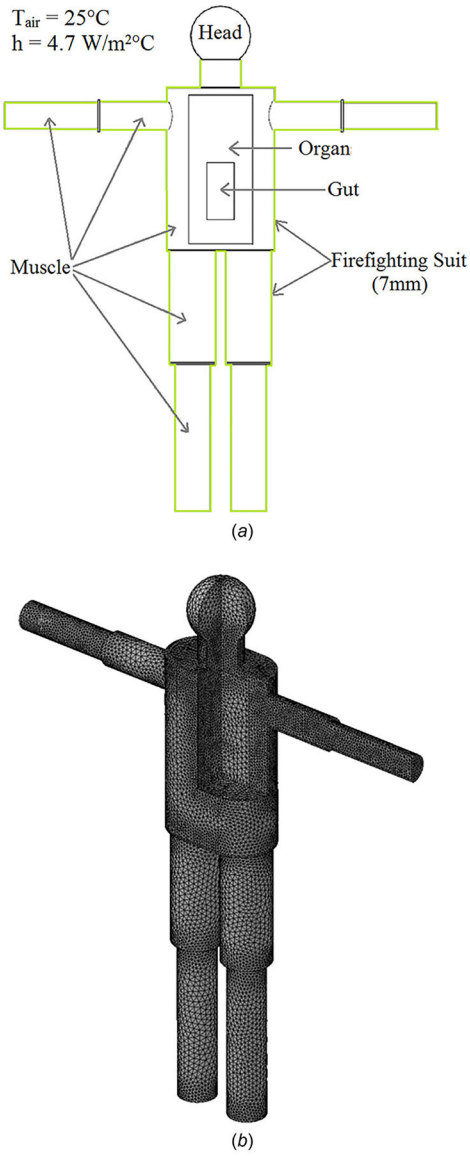

Fig. 2.

(*a*) A schematic of the 3D whole body model and (*b*) a typical mesh used for the computational simulations

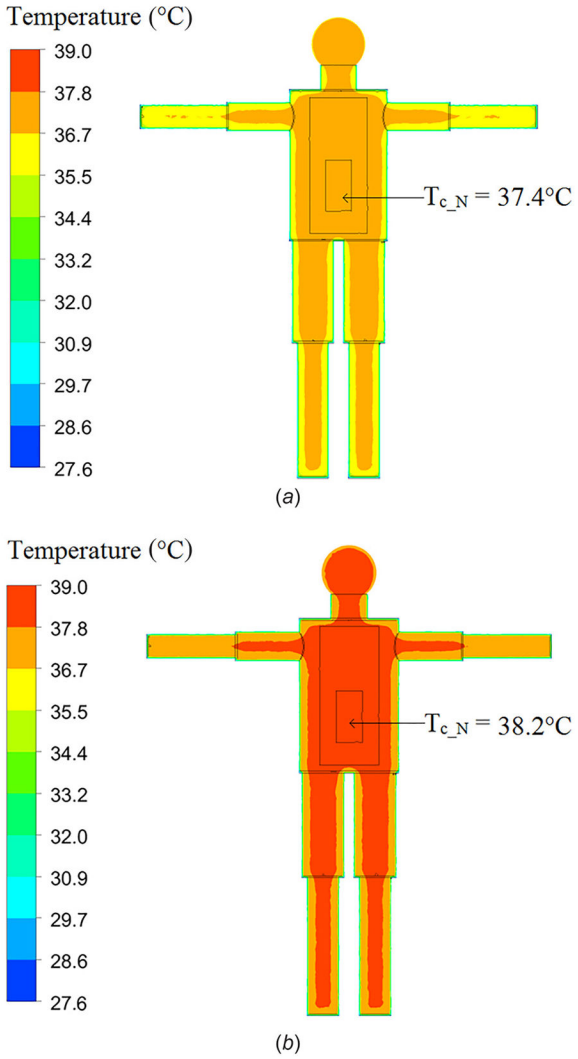

Fig. 3.

Contour plot of the whole body temperature at (*a*) steady-state and (*b*) at the end of work scenario 2 (Sc2)

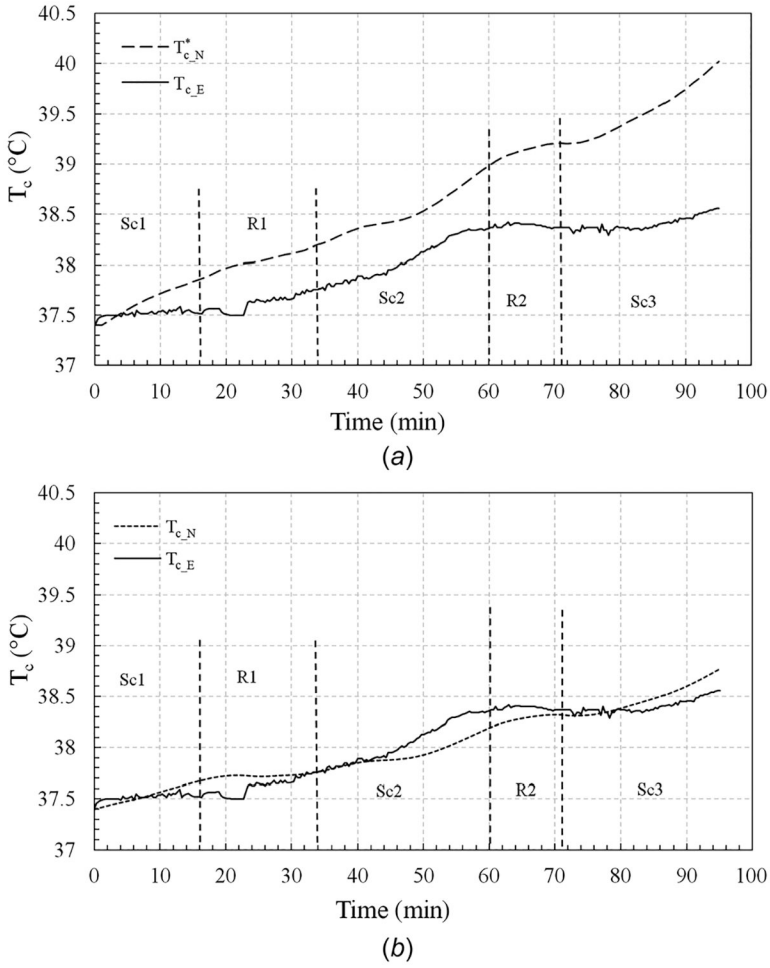

Fig. 4.

(*a*) Comparison of numerical core body temperature ($T^*_{c\_N}$) with experimental core temperature (T_{c_E}) and (*b*) comparison of T_{c_E} with core body temperature based on scaled-down metabolic rate (T_{c_N})

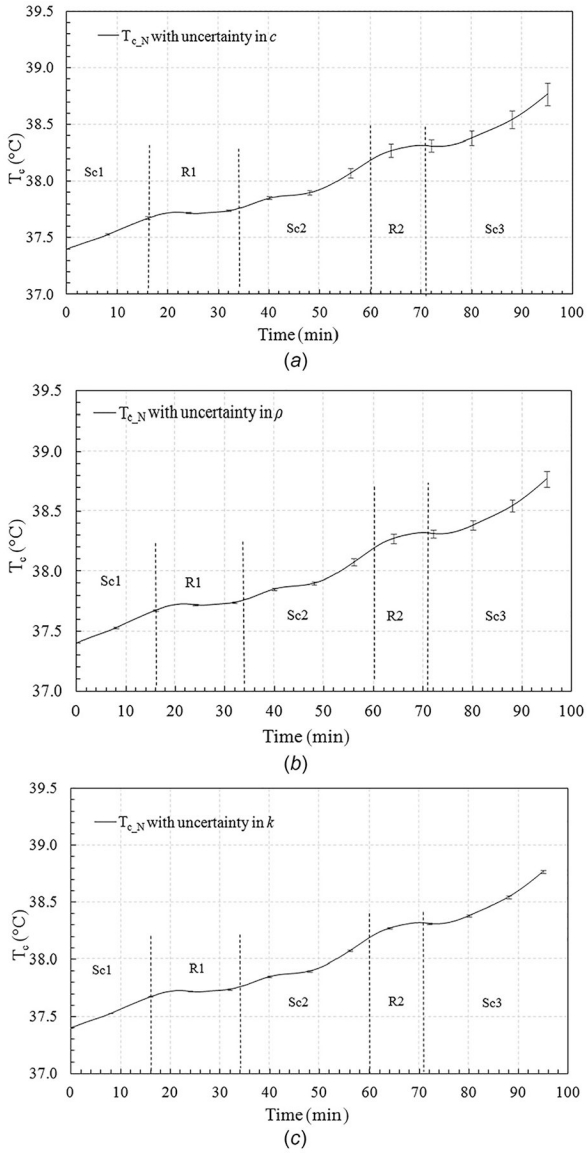

Fig. 5.

Uncertainty in T_{c_N} due to variability in (*a*) specific heat, c(*b*) density, ρ and (*c*) thermal conductivity, k

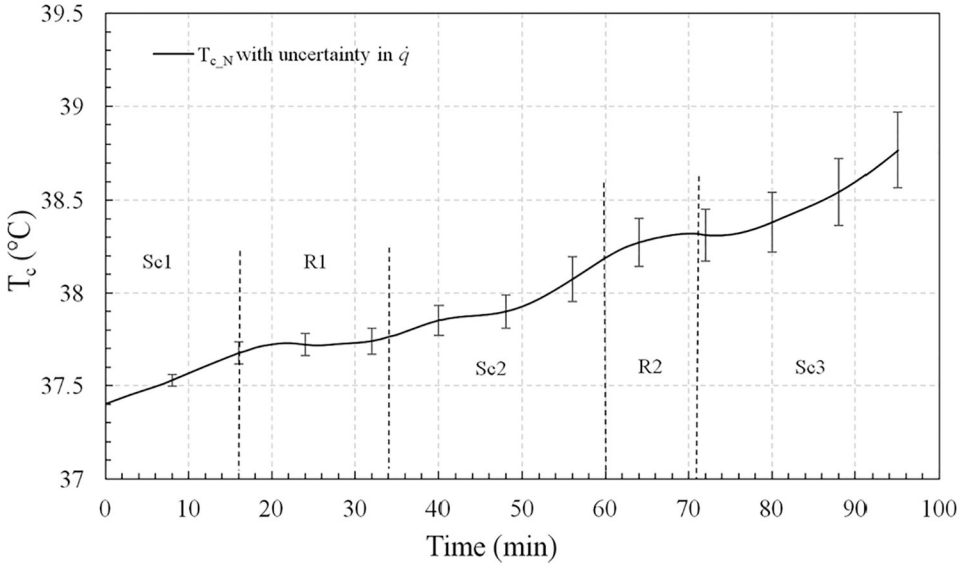

Fig. 6.

Uncertainty in T_{c_N} due variability in metabolic rate, $\dot{q}$

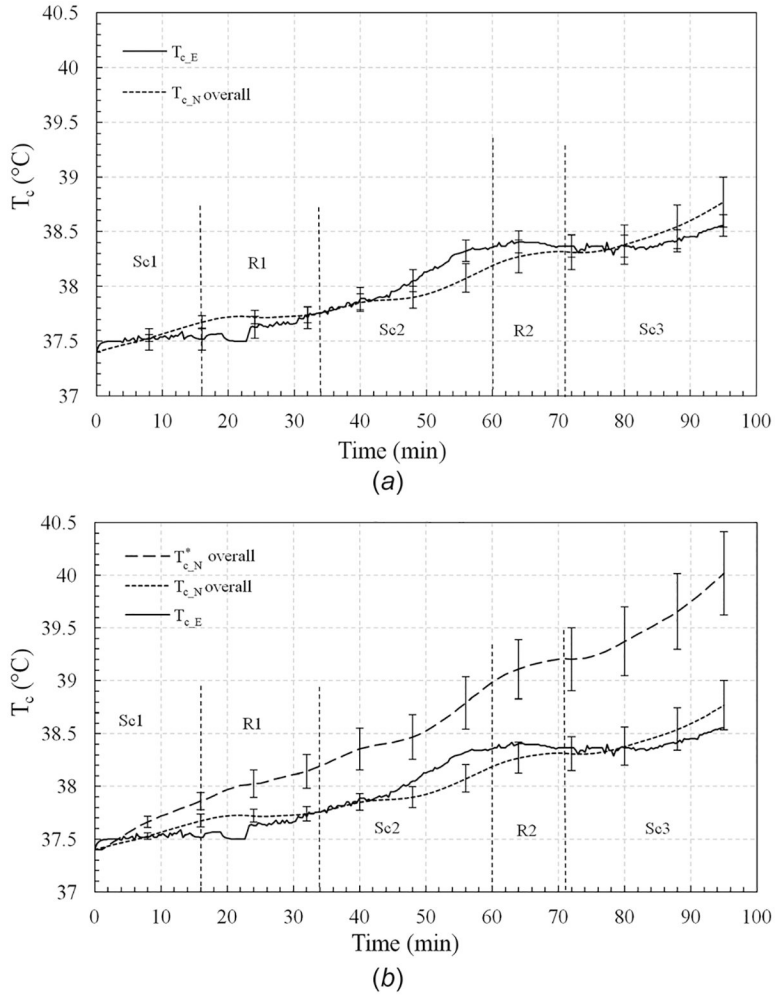

Fig. 7.

(*a*) Comparison of uncertainty in T_{c_E}, determined based on the error in temperature measurement system, with that in T_{c_n} calculated based on combined uncertainties due to variability in ρ, $\dot{q}$, c, and k and (*b*) comparison of T_{C_E} with the two numerical core temperatures (T_{c_N}, $T^*_{c\_N}$)

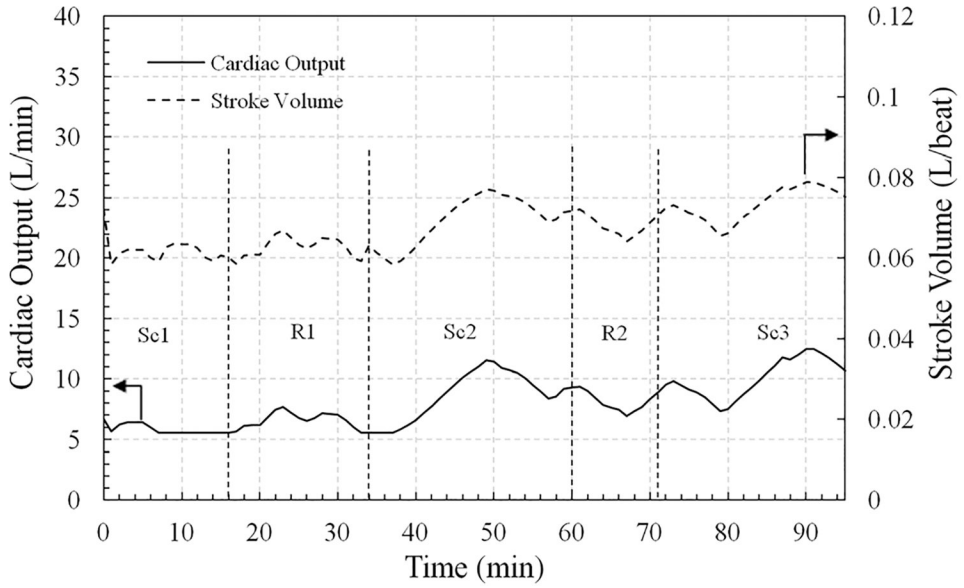

Fig. 8.
Variation of cardiac output and stroke volume during firefighting activity

Table 1

Thermal conductivity, density, and specific heat for the whole body model

Domain	Thermal conductivity, k (W/m °C) [2,4,5]	Density, ρ (kg/m^3) [2,4,12–15]	Specific heat, c (J/kg °C) [2,4,5]
		$X_n \pm \%\ u_{x_i}$	
Head	0.43 ± 6.3%	1055 ± 4.3%	3089.4 ± 6.6%
Muscle			
Organ			
Gut			

J Heat Transfer. Author manuscript; available in PMC 2019 December 06.

Table 2

Actual metabolic rate, scaled-down metabolic rate, and perfusion for the whole body model

Domain	Actual metabolic rate, $\dot{q}^*$ (W/m^3) [2,3,16,17] $X_n \pm \% u_{x_i}$	Scaled-down metabolic rate, $\dot{q}$ (W/m^3)	Blood perfusion, ω (1/s) [2,5]
Head	9865.5 ± 18.4%	6191.0 ± 18.4%	0.0045
Muscle	597.5 ± 18.4%	375.0 ± 18.4%	0.0004
Organ	4326.9 ± 18.4%	2715.3 ± 18.4%	0.0030
Gut	6994.0 ± 18.4%	4389.0 ± 18.4%	0.0082

Table 3

Properties of the blood and firefighting suit

Entity	Thermal conductivity, k (W/m °C)	Density, ρ (kg/m^3)	Specific heat, c (J/kg °C)
Firefighting suit [32,33]	0.0345	135.96	1335.4
Blood [2]	0.510	1046.00	3651.0

J Heat Transfer. Author manuscript; available in PMC 2019 December 06.